DNA 4161F

MEASUREMENTS OF DYNAMIC FRICTION BETWEEN ROCK AND STEEL

Systems, Science and Software
P.O. Box 1620
La Jolla, California 92038

25 October 1976

Final Report

CONTRACT No. DNA 001-75-C-0183

APPROVED FOR PUBLIC RELEASE; DISTRIBUTION UNLIMITED.

THIS WORK SPONSORED BY THE DEFENSE NUCLEAR AGENCY
UNDER RDT&E RMSS CODE B344076464 Y99QAXSB04806 H2590D.

Prepared for
Director
DEFENSE NUCLEAR AGENCY
Washington, D. C. 20305

Destroy this report when it is no longer needed. Do not return to sender.

UNCLASSIFIED

SECURITY CLASSIFICATION OF THIS PAGE (When Data Entered)

REPORT DOCUMENTATION PAGE

READ INSTRUCTIONS BEFORE COMPLETING FORM

1 REPORT NUMBER: DNA 4161F	2 GOVT ACCESSION NO
3 RECIPIENT'S CATALOG NUMBER	
4 TITLE (and Subtitle): MEASUREMENTS OF DYNAMIC FRICTION BETWEEN ROCK AND STEEL.	5 TYPE OF REPORT & PERIOD COVERED: Final Report.
6 PERFORMING ORG. REPORT NUMBER: SSS-R-77-3046	
7 AUTHOR(s): E. S. Gaffney	8 CONTRACT OR GRANT NUMBER(s): DNA 001-75-C-0183
9 PERFORMING ORGANIZATION NAME AND ADDRESS: Systems, Science and Software, P.O. Box 1620, La Jolla, California 92038	10 PROGRAM ELEMENT, PROJECT, TASK AREA & WORK UNIT NUMBERS: NWED Subtask Y99QAXSB048-06
11 CONTROLLING OFFICE NAME AND ADDRESS: Director, Defense Nuclear Agency, Washington, D.C. 20305	12 REPORT DATE: 25 October 1976
	13 NUMBER OF PAGES: 52 (12) 42 p.
14 MONITORING AGENCY NAME & ADDRESS (if different from Controlling Office)	15 SECURITY CLASS (of this report): UNCLASSIFIED
	15a DECLASSIFICATION DOWNGRADING SCHEDULE

16 DISTRIBUTION STATEMENT (of this Report)

Approved for public release; distribution unlimited.

DDC RECEIVED SEP 1 1977 C

17 DISTRIBUTION STATEMENT (of the abstract entered in Block 20, if different from Report)

18 SUPPLEMENTARY NOTES

This work sponsored by the Defense Nuclear Agency under RDT&E RMSS Code B344076464 Y99QAXSB04806 H2590D.

19 KEY WORDS (Continue on reverse side if necessary and identify by block number)

Dynamic Friction
Internal Friction
Physical Properties of Rocks and Soils
Earth Penetrators
Friction at High Speed

20 ABSTRACT (Continue on reverse side if necessary and identify by block number)

Instrumentation has been developed for measuring frictional forces at high velocities between rock samples and the outer rim of a rotating steel wheel. The instrumentation has been used to determine sliding friction values for volcanic tuff, wet and dry sandstone, limestone, grout, bronze and teflon. Friction in all these materials was found to obey the law $\tau = \mu\sigma e^{-c\sigma/\xi}$ where c

DD FORM 1 JAN 73 1473 EDITION OF 1 NOV 65 IS OBSOLETE

UNCLASSIFIED

SECURITY CLASSIFICATION OF THIS PAGE (When Data Entered)

388567

20. ABSTRACT (Continued)

is the sliding velocity, σ is the normal stress, τ is the tangential stress and μ and ξ are parameters dependent on the material sliding on the steel. For all rocks and rock-like materials studied, ξ was found to have a value of 2 GPa·m/s. The standard deviation of the difference between observed values and values calculated from this expression is 1.5 MPa, or 19% for all five rocks combined. Bronze and teflon were found to obey a similar relation with different values of ξ, 6.6 GPa·m/s and 0.6 GPa·m/s, respectively. For the limited sample available, ξ appears to be related to the thermal conductivity. For the five rocks, μ is decreased by the presence of volatile components such as H_2O and CO_2.

Attempts to measure friction values for soil in the test device used for this program were unsuccessful due to insufficient cohesion in the soils. A friction rule for soil is suggested based on extrapolation of rock behavior and static friction measurements.

TABLE OF CONTENTS

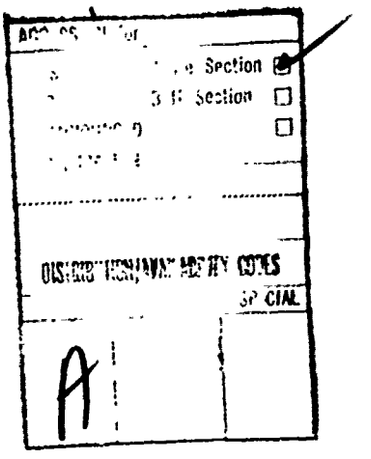

LIST OF ILLUSTRATIONS

LIST OF TABLES

I. INTRODUCTION

In recent years the Defense Nuclear Agency (DNA) has sponsored research concerning the loading and response of projectiles during earth penetration as part of its Earth Penetrating Weapons Technology Program. These studies have been designed to increase our understanding of the process of penetration of earth materials by high velocity projectiles. This work has included numerical computer modeling of the penetration process, experimental simulation of penetration, and experimental investigation of phenomenology related to penetration. One of the phenomena considered to be important in proper simulation or modeling of the penetration process is the friction that exists between the high velocity steel penetrator and the rock or soil material that it is penetrating. Very little previous work has been done to determine friction coefficients between rock and steel at velocities in excess of 5 m/s and high normal stresses. As a consequence, Systems, Science and Software (S^3) has undertaken an experimental investigation for DNA, of frictional forces between rock and steel at high sliding velocity (up to 30 m/s) and high normal stresses.

An existing rotary viscometer, developed for DNA under a previous contract, was modified to measure frictional stresses. The details of this device and its instrumentation have been reported in a previous report[1]. However, for convenience, a brief description of the instrumentation and its operation is given in Section II. In Section III of this report the data that has been obtained on five rocks and two other materials is presented. Section IV discusses the results and their implications for earth penetrating vehicles.

II. TEST EQUIPMENT AND INSTRUMENTATION

We have modified a rotary viscometer (developed for DNA under contract DNA001-74-C-0077) to permit measurement of friction between rock samples and a flywheel of low carbon (1020) steel. The arrangement is shown schematically in Figure 2.1. The wheel is set rotating with no load on the wheel. When the wheel has reached the desired rotational speed two rock samples are pressed onto opposite radii of the flywheel for about 200 msec. This load duration was chosen so that the load could reach a steady value and so that the sample would be sliding on a fresh surface for the lowest initial velocities used (10 m/s). The normal and tangential loads are measured during this event. Data from all four load cells are recorded on an oscilloscope. The rotational velocity is measured by a photodetector which looks at a pattern attached to the axis of the flywheel. This pattern repeats ten times per revolution. The test interval ranged from a half to one and a half revolutions. The photodetector output is also recorded on an oscilloscope. Figure 2.2 shows a typical set of raw data. Data presented in this report are taken from the first 50 msec of the recorded traces so that they refer to a fresh steel surface. After each test the wheel was resurfaced without lubrication using a corundum grinder.

III. RESULTS

S^3 has used the instrumentation described above to measure frictional properties of five rocks, bronze and teflon sliding on steel at velocities between 10 and 30 m/s. The materials studied are described in Table 3.1. Data, in the form of sliding velocity (c), normal stress* (σ) and tangential stress (τ), are shown in Table 3.2 for tuff from the Tonopah Test Range (TTR); in Table 3.3 for dry Dakota sandstone; in Table 3.4 for wet Dakota sandstone; in Table 3.5 for Solenhofen

*These are average stresses, i.e., total force ÷ sample area.

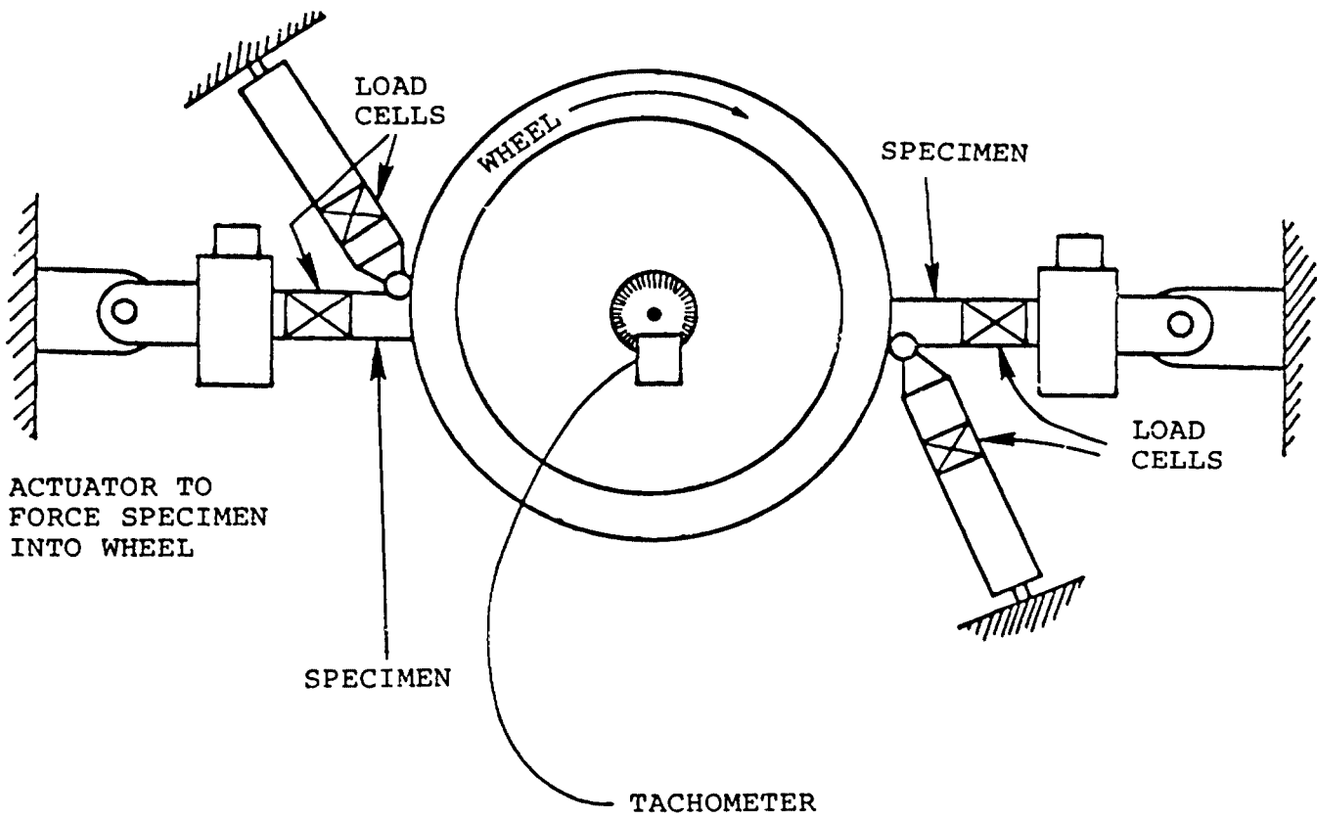

Figure 2.1 Test apparatus for rock-on-steel friction measurements.

(a) Sample J/11

Upper Trace
Normal Load
2 V/div ≅ 35.6 kN/div

Lower Trace
Tangential Load
1 V/div ≅ 17.8 kN/div

50 ms/div

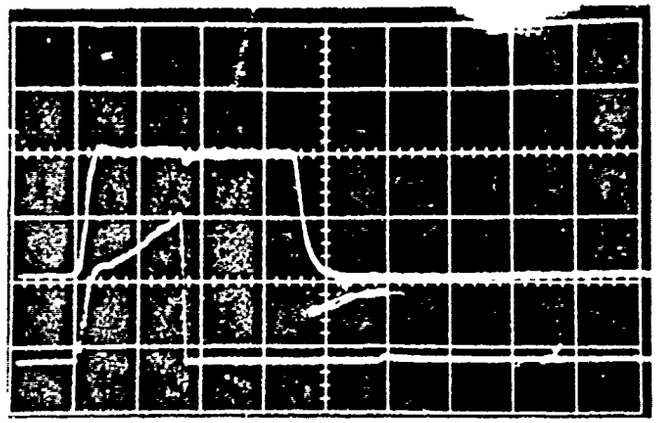

(b) Sample N/7

Upper Trace
Normal Load
2 V/div ≅ 35.6 kN/div

Lower Trace
Tangential Load
1 V/div ≅ 17.8 kN/div

50 ms/div

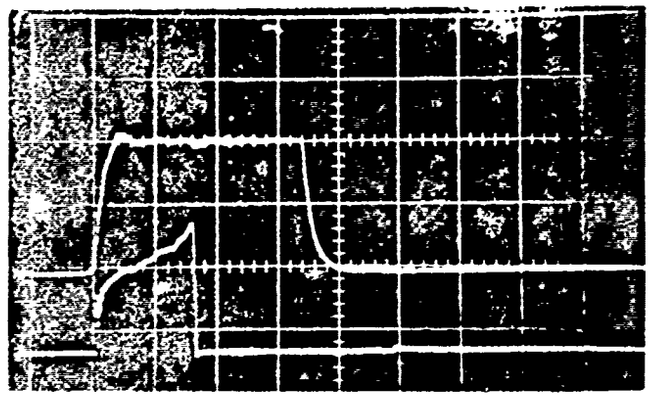

(c) Velocity

Tachometer Output
1 cycle = 1/10 rev
Sweep Rate = 50 ms/div

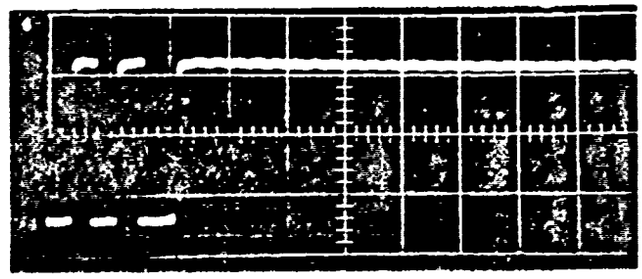

Figure 2.2 Typical raw data records. C_o = 10 m/s; normal load, 6.7 MPa.

Table 3.1 Description of materials tested.

Tuff[a]	A welded tuff from the Tonopah Test Range, Nevada. Aphanitic to glassy matrix with several percent lithic fragments and feldspar clasts, ρ ~2.6 g/cm^3.
Sandstone[a,b]	A quartz sandstone from the Dakota formation near San Ysidro, New Mexico. Porosity ~20%, ρ ~2.2 gm/cm^3. "Dry" samples were air dried for several days. "Wet" samples were soaked in water overnight, mounted in test cell less than 5 minutes before test.
Limestone	Lithographic limestone from Solenhofen, Germany, ρ = 2.6 gm/cm^3.
Grout[b]	Sand-cement mix formulated by AVCO Corp.
Bronze	660 bronze 83% Cu, 7% Sn, 7% Pb, 3% Zn.
Teflon	Polytetrafluorethylene.

[a]From the site of full-scale DNA projectile penetration field tests.

[b]Typical of targets used in half-scale DNA reverse ballistic penetration experiments.

Table 3.2 Raw friction data for welded tuff sliding on steel.

Test No.	c (m/s)	σ (MPa)	τ (MPa)
75F10	10	12.5	7.2
		13.4	7.5
75F15	10	11.2	4.8
75F18	10	30.0	13.2
75F22	10	66.3	26.5
		69.5	24.3
75F11	20	13.4	5.6
		13.4	5.4
75F14	20	11.6	4.4
		8.5	3.1
75F17	20	49.8	13.9
		45.7	14.6
75F21	20	65.4	17.0
		64.1	16.0
75F12	30	14.3	5.7
		14.3	6.0
75F13	30	16.1	8.1
		16.6	6.0
75F16	30	45.2	13.1
		43.9	12.3
75F19	30	33.9	8.7
75F20	30	55.1	12.7
		52.0	12.0
76F47	30	107.0	11.4

Table 3.3 Raw friction data for dry sandstone sliding on steel.

Test No.	c (m/s)	σ (MPa)	τ (MPa)
76F01	11	13	4.6 5.6
76F04	10	23	5.8 8.5
76F07	12	47	14.1 17.4
76F02	20	15	4.8 4.2
76F05	23	29	9.6 6.6
76F08	20	59	8.9 7.1
76F03	32	15	6.3
76F06	32	22	7.0 6.6
76F09	32	46	10.1 11.5

Table 3.4 Raw friction data for wet sandstone sliding on steel.

Test No.	c (m/s)	σ (MPa)	τ (MPa)
76F22	10	14.3	3.8
	10	13.7	6.1
76F24	10	15.7	4.7
76F27	9.7	34.5	14.3
	9.7	40.6	13.7
76F20	20	17.2	3.0
76F25	20	21.9	5.7
	20	25.1	5.9
76F28	19	61.1	10.9
76F21	31	18.3	4.0
	31	16.7	3.3
76F26	31	30.5	5.3
76F29	30	51.7	10.0

Table 3.5 Raw friction data for limestone sliding on steel.

Solenhofen limestone

Test No.	c (m/s)	σ (MPa)	τ (MPa)
76F48	29.3	13.4	1.5
		15.7	1.1
76F50	29.3	38.5	4.6
		37.6	3.6
76F52	29.4	43.9	3.0
		47.0	2.5
76F49	14.8	36.6	4.6
		42.3	3.8
76F51	14.8	76.9	7.4
		81.4	5.3

limestone; in Table 3.6 for sand-cement grout; in Table 3.7 for 660 bronze; and in Table 3.8 for teflon (polytetrafluoroethylene). The data are also presented graphically in Figures 3.1 through 3.6, respectively. Some of the data on tuff and dry sandstone have been reported previously[1].

Attempts to measure the frictional properties of two soils, Buckshot clay and clay from White Sands missile range, proved unsuccessful due to the very low strength of the soils. Specimens of all the soil and all the rock materials except Solenhofen limestone were supplied by Waterways Experiment Station (WES). The limestone was provided by Dr. Karl Schuler of Sandia Laboratories and machined by WES.

IV. DISCUSSION

4.1 A General Friction Law

In the earlier report[1], we demonstrated that all of the frictional data on TTR tuff obtained for normal stresses below 70 MPa could be explained with a linear dependence of τ on σ with the friction coefficient μ decreasing as the sliding velocity increased. During the last year's contract effort, one additional measurement was made with TTR tuff sliding on steel at a velocity of 30 m/s and a normal stress of over 100 MPa. The results of this experiment did not follow the same relations as the lower stress tests. As a result we must find a new relation between the tangential stress τ, and the normal stress σ.

Such a relation was suggested by D. K. Butler of the WES[2]. Butler suggested a friction law of the form

$$\tau = \tau_o + \mu\sigma\, e^{-\sigma/\sigma^*} \qquad (1)$$

where τ_o and σ^* are constants with units of stress.

Table 3.6 Raw friction data for sand-cement grout sliding on steel.

Test No.	c (m/s)	σ (MPa)	τ (MPa)
76F13	10	29	7.8
		26	6.2
76F16	10	46	10.6
76F11	22	13	4.9
		13	5.1
76F14	21	33	9.9
		33	7.6
76F17	20	42	7.6
		42	8.8
76F12	33	14	4.9
		14	4.5
76F15	30	30	6.0
		30	6.3

Table 3.7 Raw friction data for bronze sliding on steel.

Test No.	c (m/s)	σ (MPa)	τ (MPa)
76F37	20	35.1	4.2
76F38	20	34.0	4.1
76F39	20	44.5	4.5
76F40	20	41.0	5.3
76F41	20	45.7	6.5
76F42	20	296.0	14.8

Table 3.8 Raw friction data for teflon sliding on steel.

Test No.	c (m/s)	σ (MPa)	τ (MPa)
76F43	20	13.9	1.7
76F44	20	23.6	1.9
76F45	20	36.3	2.1
76F46	20	44.2	2.1

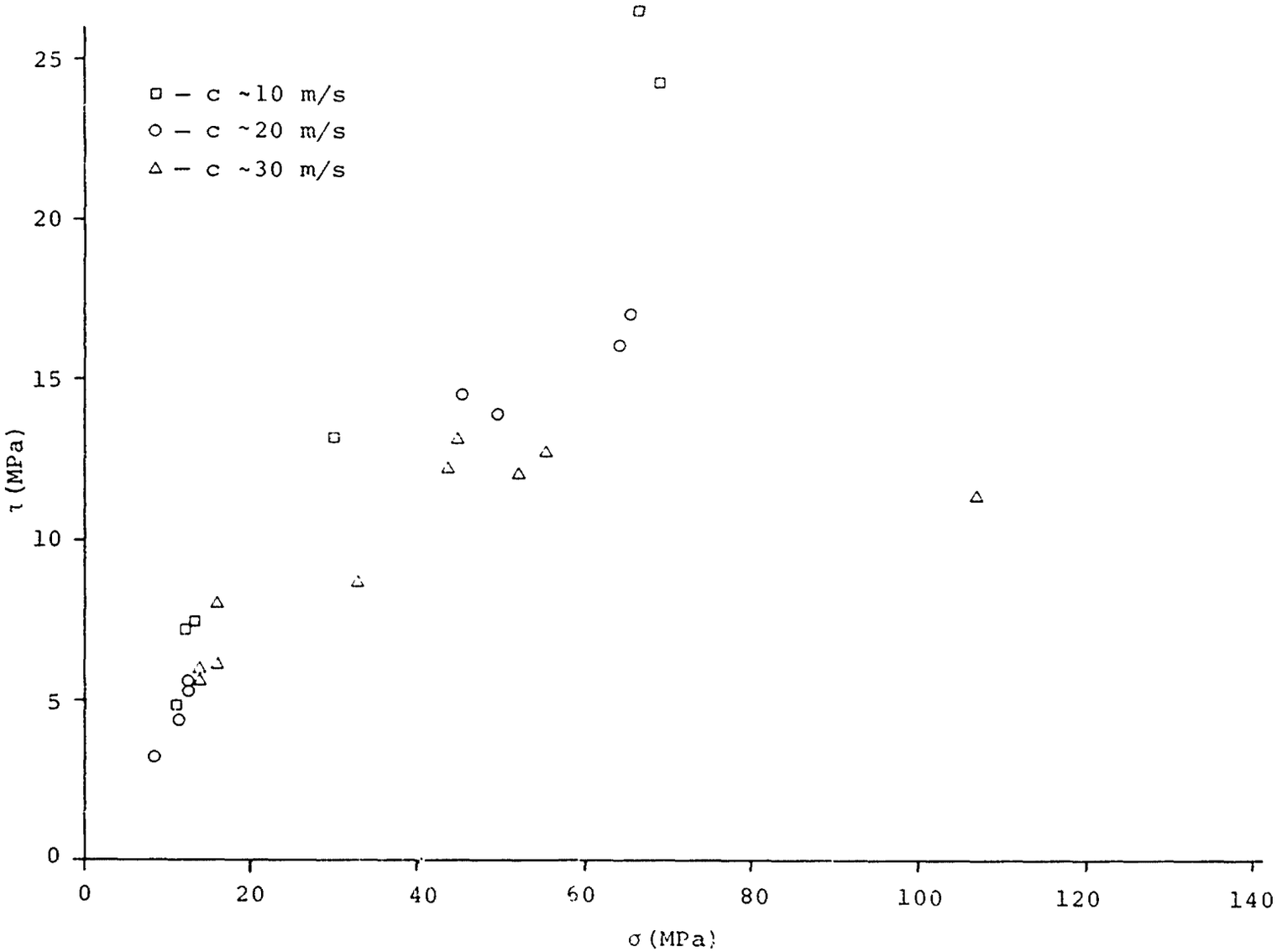

Figure 3.1 Frictional data for TTR tuff sliding on steel.

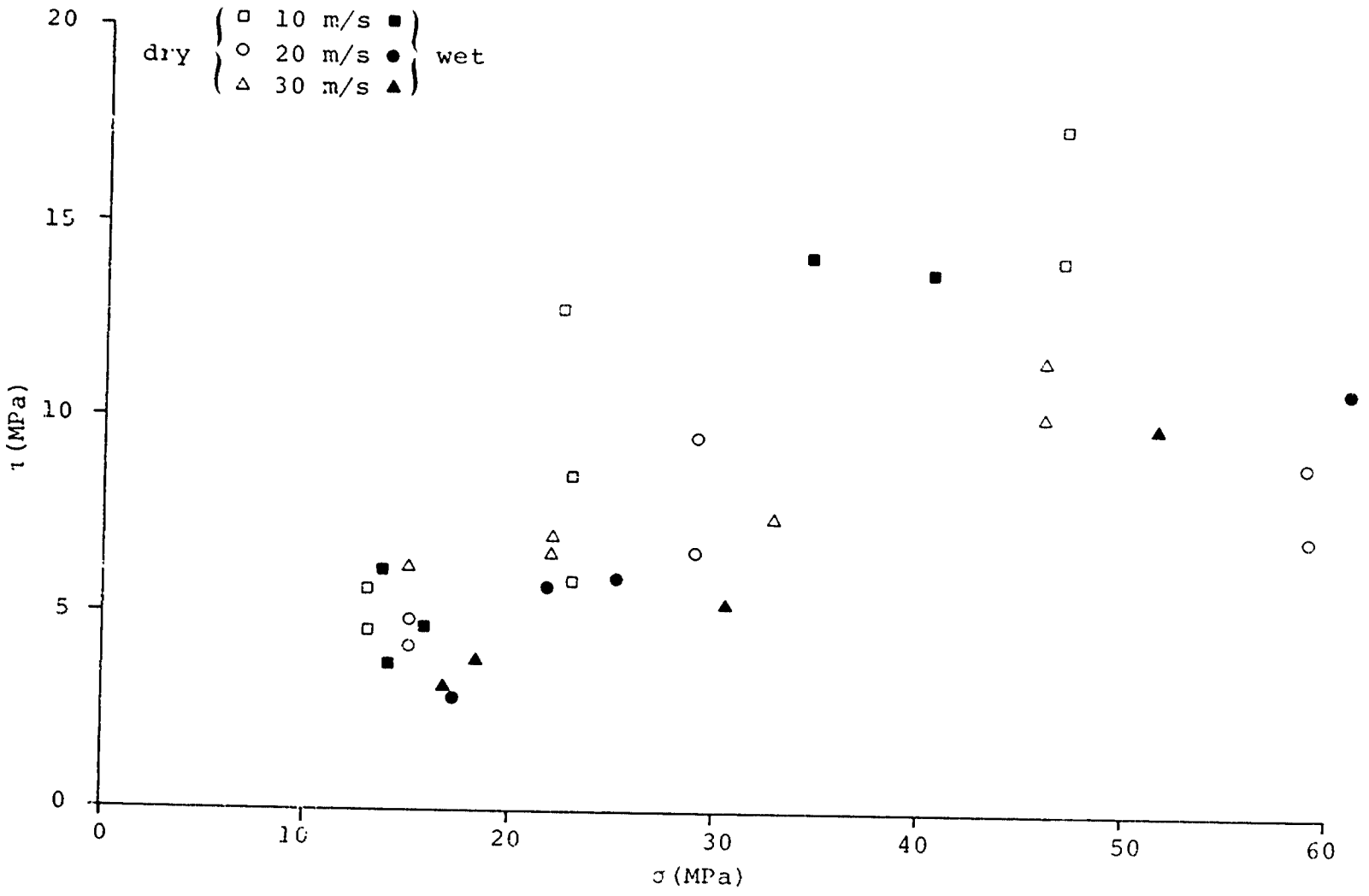

Figure 3.2 ...ctional data for sandstone sliding on steel. Symbols as in ...igure 3 1 except that open symbols are for dry sandstone; closed symbo... for wet sandstone.

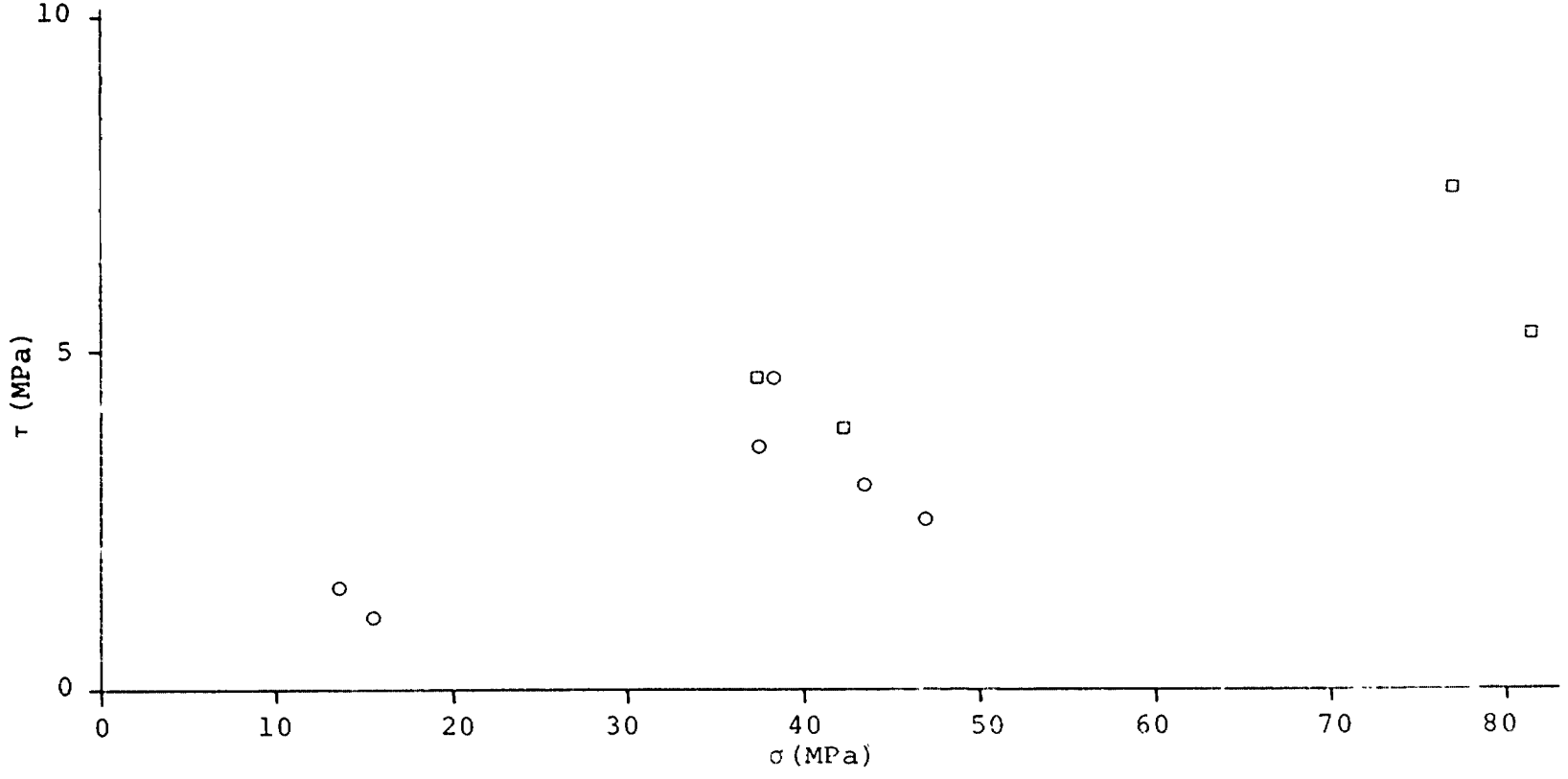

Figure 3.3 Frictional data for Solenhofen limestone. Symbols as in Figure 3.1.

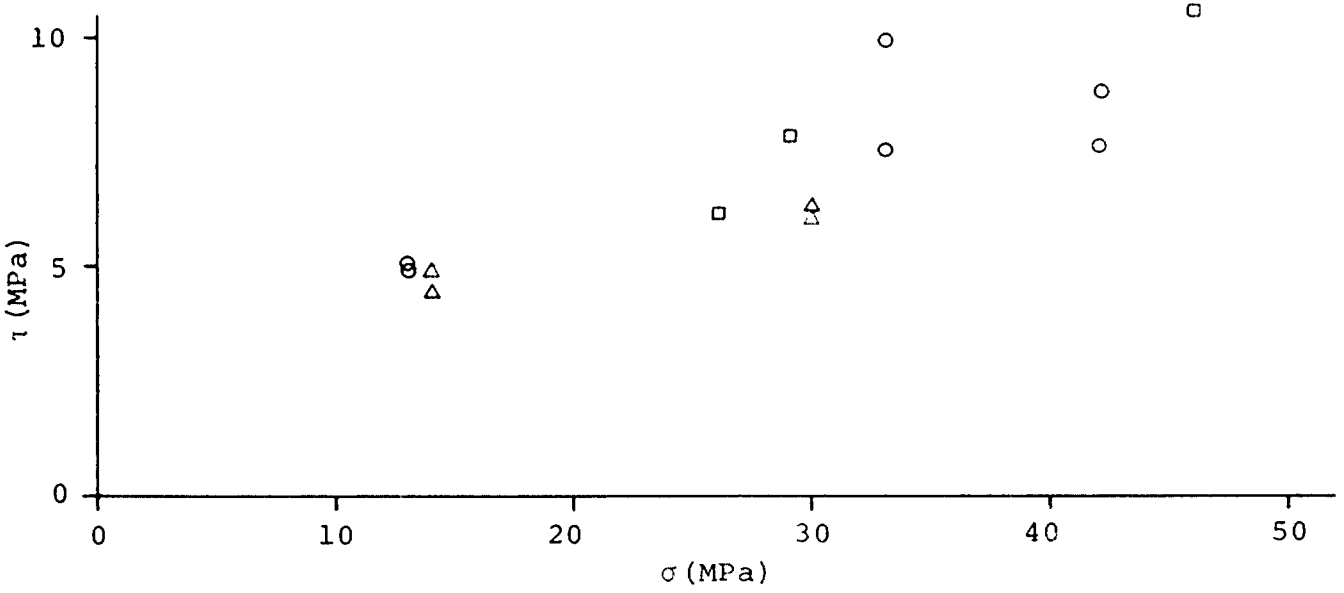

Figure 3.4 Frictional data for sand-cement grout. Symbols as in Figure 3.1.

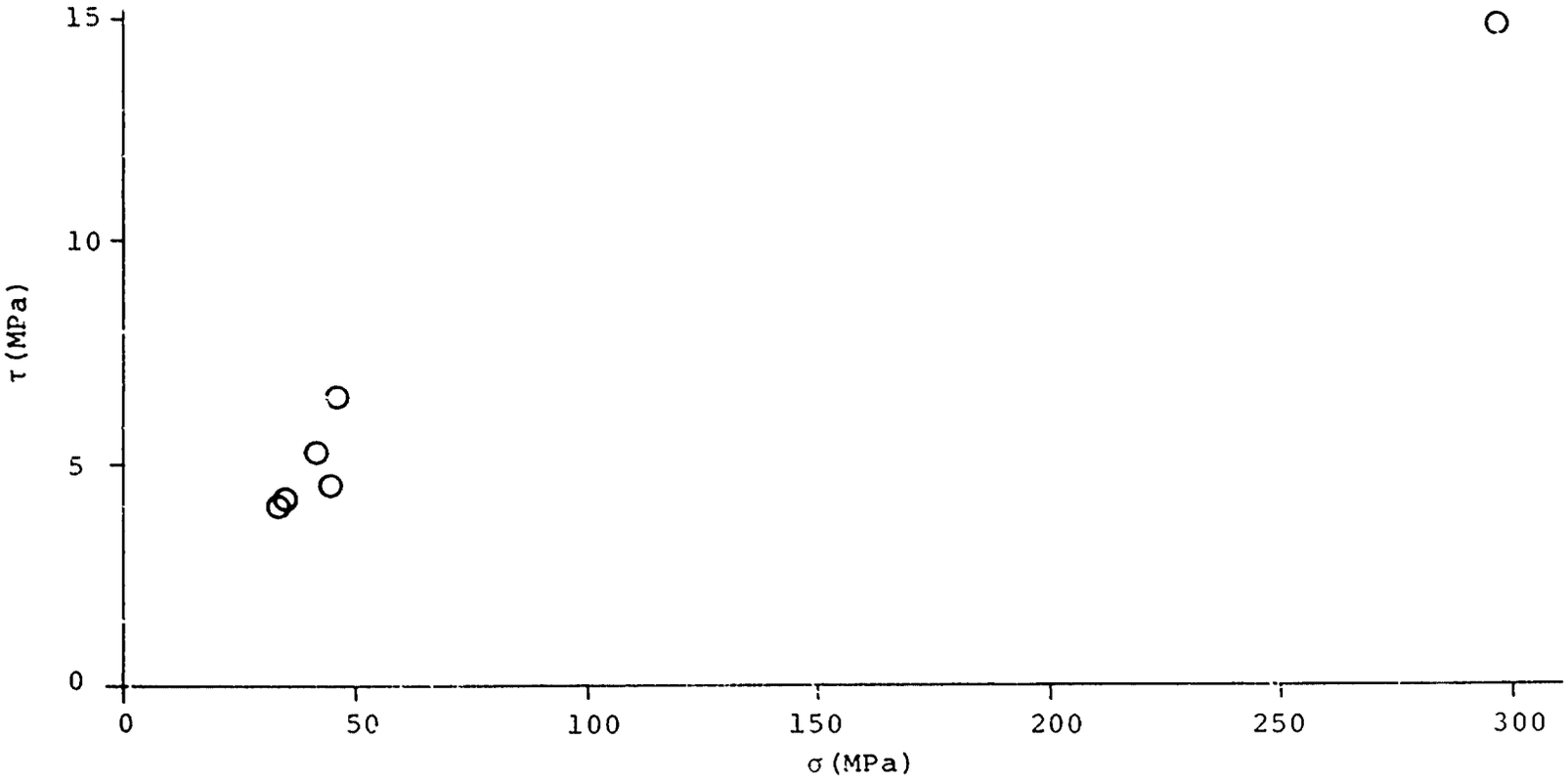

Figure 3.5 Frictional data for 660 bronze. Symbols as in Figure 3.1.

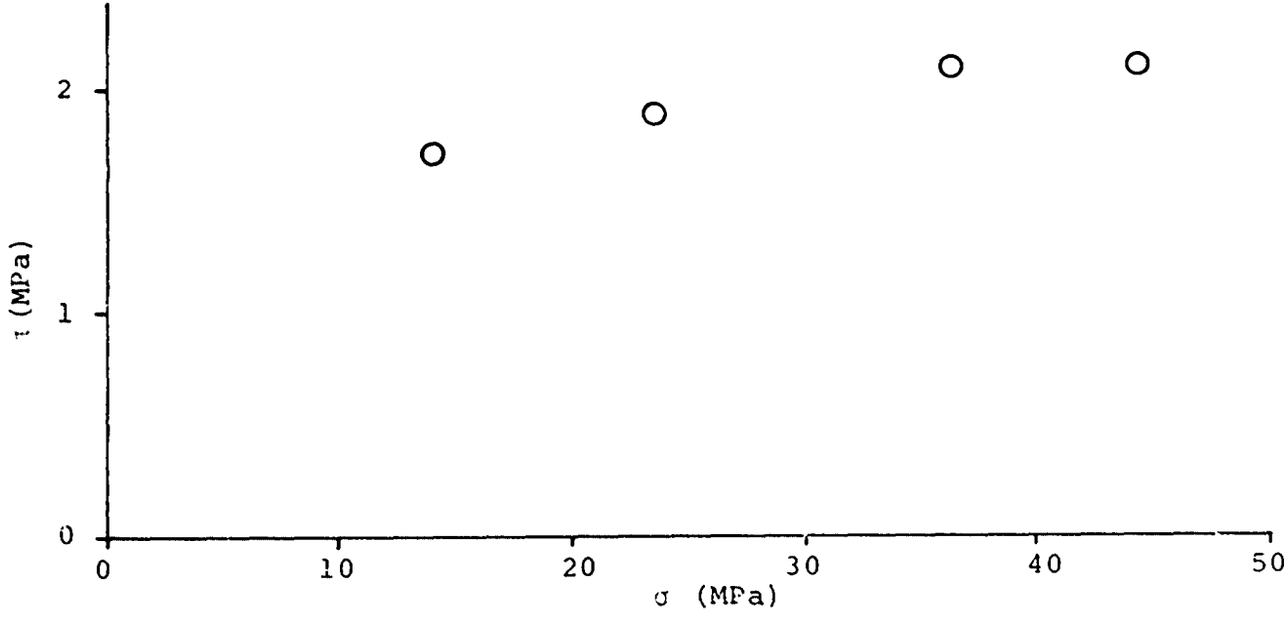

Figure 3.6 Frictional data for teflon. Symbols as in Figure 3.1.

Attempts to apply this relationship to the data obtained on TTR tuff worked quite well for any given sliding speed. However, it was found that the value of σ^* best suited to each sliding velocity varied proportional to the sliding velocity. A zero value for τ_o fit the data well. Therefore, we have empirically modified the relationship and used the general form

$$\tau = \mu\sigma\, e^{-c\sigma/\xi} \qquad (2)$$

where σ is the normal stress, c the sliding velocity, τ the tangential stress and μ and ξ are material-dependent parameters.

Application of Equation (2) to the data results in reduction of data from all sliding velocities to a single linear relation

$$\tau = \mu\sigma_{eff} \qquad (3)$$

where $\sigma_{eff} = \sigma e^{-c\sigma/\xi}$. For a value of ξ equal to 2.0 GPa m/s, the recast data for TTR tuff are shown in Figure 4.1. A straight line of slope 0.5 has been drawn through the data. The standard deviation of the differences between the observed values of τ and those indicated for the linear dependence is 1.04 MPa.

Encouraged by these results, we attempted to apply the analysis to other materials. Values of μ and ξ found to give good fits to the data are shown in Table 4.1. Also shown is the standard deviation of the difference between observed tangential forces and those calculated using Equation (2) and the values of Table 4.1. The values of all parameters were chosen by inspection and are not the result of a least squares or similar curve-fitting procedure. Furthermore, the value ξ used for all rocks and rock-like materials was chosen to be the same as that used for TTR tuff. Although this choice is somewhat arbitrary, changing ξ from 2.0 to 1.5 GPa•m/s does not have a significant effect on the standard deviation of the difference between calculated and observed

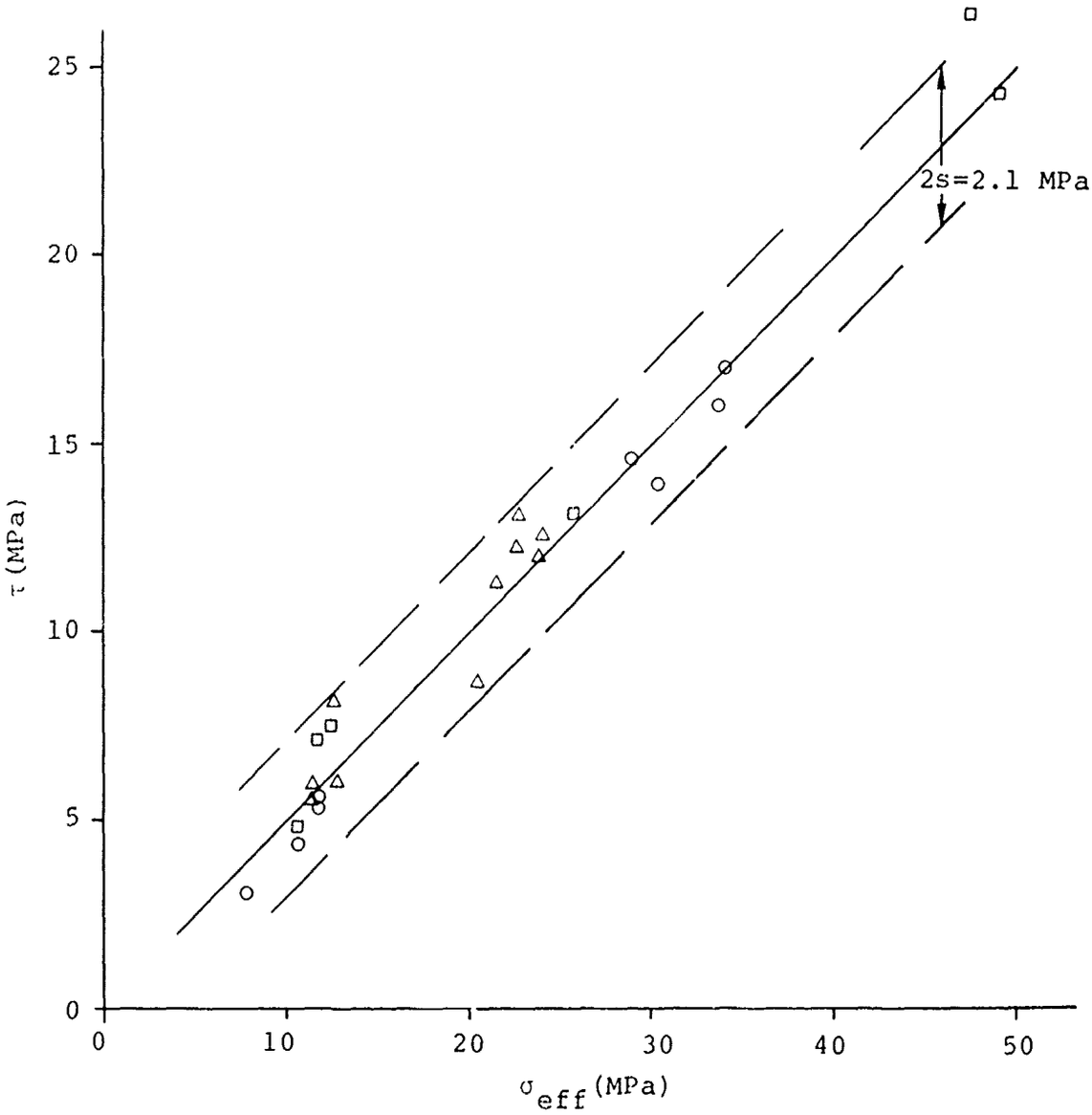

Figure 4.1 Frictional data for welded tuff recast in terms of σ_{eff}. Symbols as in Figure 3.1.

Table 4.1 Frictional properties of rocks and other materials studied.

ROCK	μ	ξ (GPa·m/s)	s^* (MPa)
Tuff	.50	2.0	1.04
Sandstone (Dry)	.39	2.0	2.33
Sandstone (Wet)	.34	2.0	1.83
Limestone	.14	2.0	0.88
Grout	.34	2.0	1.17
Bronze	.13	6.6	0.80
Teflon	.20	0.6	0.13

*s = Standard deviation of $\tau_{calc} - \tau$.

values of τ. However, it does result in a marked change in the μ which must be used to best fit the observed data. The linearized data for all materials studied are presented in Table 4.2 and shown graphically in Figures 4.2 through 4.7.

It was found that data for bronze and teflon could not be fit with a value of ξ of 2 GPa·m/s. For teflon a lower value of 0.6 GPa·m/s was required to obtain a reasonable fit to the observed data. For bronze a much higher value of 6.6 GPa·m/s was used. With these values of ξ, good fits to all of the observed data were obtained.

4.2 Significance of the Factor ξ

The factor ξ used in the exponential relationship to convert from observed normal stress, σ, to effective normal stress, σ_{eff}, has the units of pressure times velocity. Alternatively, it may be expressed in terms of energy per unit area per unit time, or power per unit area. This dimensionality of ξ suggests that it should be related to the power dissipation at the sliding interface.

Although accurate values of thermal conductivity are not available for any of the materials studied, we can estimate conductivities based on literature values. Taking values of 6×10^{-4}, 6×10^{-3} and 0.45 $(cal/cm^2\text{-sec})/(deg/cm)$ for the teflon, a "typical" rock, and bronze, respectively, we find that the values of ξ (0.6, 2 and 6.6 GPa·m/s, respectively) increase with the thermal conductivity of the sample. It is exactly what we would expect if ξ were indeed a power per unit area lost at the sliding surface and if the loss were controlled by thermal conductivity into the sample. In fact, energy produced at the interface is lost both to the sample and to the wheel, and to the air through ablation. Since conductivity of steel is much greater than that of rock, essentially all conductive heat must be lost to steel. Heat is also lost by ablation, which is probably the greatest heat sink. Thus, the relation of ξ to thermal conductivity may not be meaningful.

Table 4.2 Friction data recast in the form

$$\sigma_{eff} = \sigma \exp(-c\sigma/\xi), \quad \tau_{calc} = \mu \sigma_{eff}$$

Test No.	c (m/s)	σ (MPa)	σ_{eff} (MPa)	τ (MPa)	τ_{calc} (MPa)	Material
75F10	10	12.5	11.7	7.2	5.9	Tuff ξ = 2.0 GPa·m/s μ = 0.50
		13.4	12.5	7.5	6.2	
75F15	10	11.2	10.6	4.8	5.3	
75F18	10	30.0	25.8	13.2	12.9	
75F22	10	66.3	47.6	26.5	23.8	
		69.5	49.1	24.3	24.6	
75F11	20	13.4	11.7	5.6	5.9	
		13.4	11.7	5.4	5.9	
75F14	20	11.6	10.3	4.4	5.1	
		8.5	7.8	3.1	3.9	
75F17	20	49.8	30.3	13.9	15.1	
		45.7	28.9	14.6	14.4	
75F21	20	65.4	34.0	17.0	17.0	
		64.1	33.8	16.0	16.9	
75F12	30	14.3	11.5	5.7	5.8	
		14.3	11.5	6.0	5.8	
75F13	30	16.1	12.6	8.1	6.3	
		16.6	12.9	6.0	6.4	
75F16	30	45.2	22.9	13.1	11.4	
		43.9	22.7	12.3	11.3	
75F19	30	33.9	20.4	8.7	10.2	
75F20	30	55.1	24.1	12.7	12.0	
		52.0	23.8	12.0	11.9	
76F47	30	107.0	21.5	11.4	10.8	

Table 4.2 (continued)

Test No.	c (m/s)	σ (MPa)	σ_{eff} (MPa)	τ (MPa)	τ_{calc} (MPa)	Material
76F22	10	14.3	13.3	3.8	4.5	
	10	13.7	12.8	4.4	6.1	
76F24	10	15.7	14.5	4.7	4.9	
70F27	9.7	34.5	29.2	14.3	9.9	
	9.7	40.6	33.3	13.7	11.3	
76F20	20	17.2	14.5	3.0	4.9	Wet Sandstone
76F25	20	21.9	17.6	5.7	6.0	ξ = 2.0 GPa·m/s
	20	25.1	19.5	5.9	6.6	
76F28	19	61.1	34.2	10.9	11.6	μ = 0.34
76F21	31	18.3	13.8	4.0	4.7	
	31	16.7	12.9	3.3	4.4	
76F26	31	30.5	19.0	5.3	6.5	
76F29	30	51.7	23.8	10.0	8.1	
76F01	11	13	12.1	4.6	4.7	
	11	13	12.1	5.6	4.7	
76F04	10	23	20.5	5.8	8.0	
	10	23	20.5	8.5	8.0	
76F07	12	47	35.5	14.1	13.8	
	12	47	35.5	17.4	13.8	
76F02	20	15	12.9	4.8	5.0	Dry Sandstone
	20	15	12.9	4.2	5.0	
76F05	23	29	20.8	9.6	8.1	ξ = 2.0 GPa m/s
	23	29	20.8	6.6	8.1	μ = 0.39
76F08	20	59	32.7	8.9	12.8	
	20	59	32.7	7.1	12.8	
76F03	32	15	11.8	6.3	4.6	
76F06	32	22	15.5	7.0	6.0	
	32	22	15.5	6.6	6.0	
76F09	32	46	22.0	10.1	8.6	
	32	46	22.0	11.5	8.6	

Table 4.2 (continued)

Test No.	c (m/s)	σ (MPa)	σ_{eff} (MPa)	τ (MPa)	τ_{calc} (MPa)	Material
76F48	29.3	13.4	11.0	1.5	1.5	
		15.7	12.5	1.1	1.8	
76F50	29.3	38.5	21.9	4.6	3.1	Limestone
		37.6	21.7	3.6	3.0	
76F52	29.4	43.9	23.0	3.0	3.2	ξ = 2.0 GPa·m/s
		47.0	23.6	2.5	3.3	μ = 0.14
76F49	14.8	36.6	27.9	4.6	3.9	
		42.3	30.9	3.8	4.3	
76F51	14.8	76.9	43.5	7.4	6.1	
		81.4	44.6	5.3	6.2	
76F13	10	29	25.1	7.8	8.5	
		26	22.8	6.2	7.8	
76F16	10	46	36.5	10.6	12.4	
76F11	22	13	11.3	4.9	3.8	
		13	11.	5.1	3.8	Grout
76F14	21	33	23.3	9.9	7.9	ξ = 2.0 GPa·m/s
		33	23.3	7.6	7.9	μ = 0.34
76F17	20	42	27.6	7.6	9.4	
		42	27.6	8.8	9.4	
76F12	33	14	11.1	4.9	3.8	
		14	11.1	4.5	3.8	
76F15	30	30	19.1	6.0	6.5	
		30	19.1	6.3	6.5	

Table 4.2 (continued)

Test No.	c (m/s)	σ (MPa)	σ_{eff} (MPa)	τ (MPa)	τ_{calc} (MPa)	Material
76F37	20	35.1	31.6	4.2	4.1	Bronze ξ = 6.6 GPa m/s μ = 0.13
76F38	20	34.0	30.7	4.1	4.0	
76F39	20	44.5	38.9	4.5	5.1	
76F40	20	41.0	36.2	5.3	4.7	
76F41	20	45.7	39.8	6.5	5.2	
76F42	20	296.0	121.0	14.8	15.7	
76F43	20	13.9	8.7	1.7	1.7	Teflon ξ = 0.6 GPa m/s μ = 0.20
76F44	20	23.6	10.7	1.9	2.1	
76F45	20	36.3	10.8	2.1	2.1	
76F46	20	44.2	10.1	2.1	2.0	

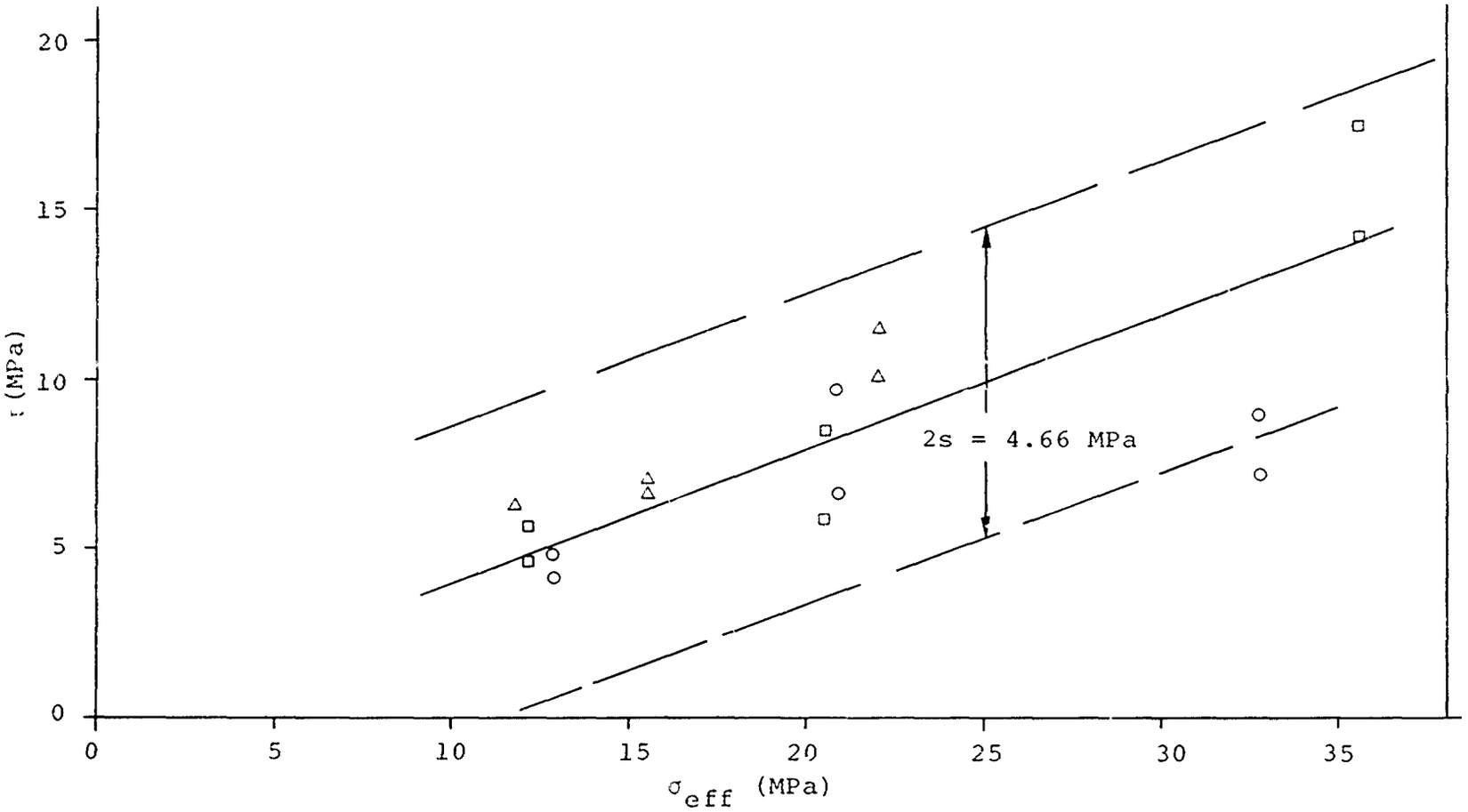

Figure 4.2 Friction data for dry sandstone recast in terms of σ_{eff}. Symbols as in Figure 3.2.

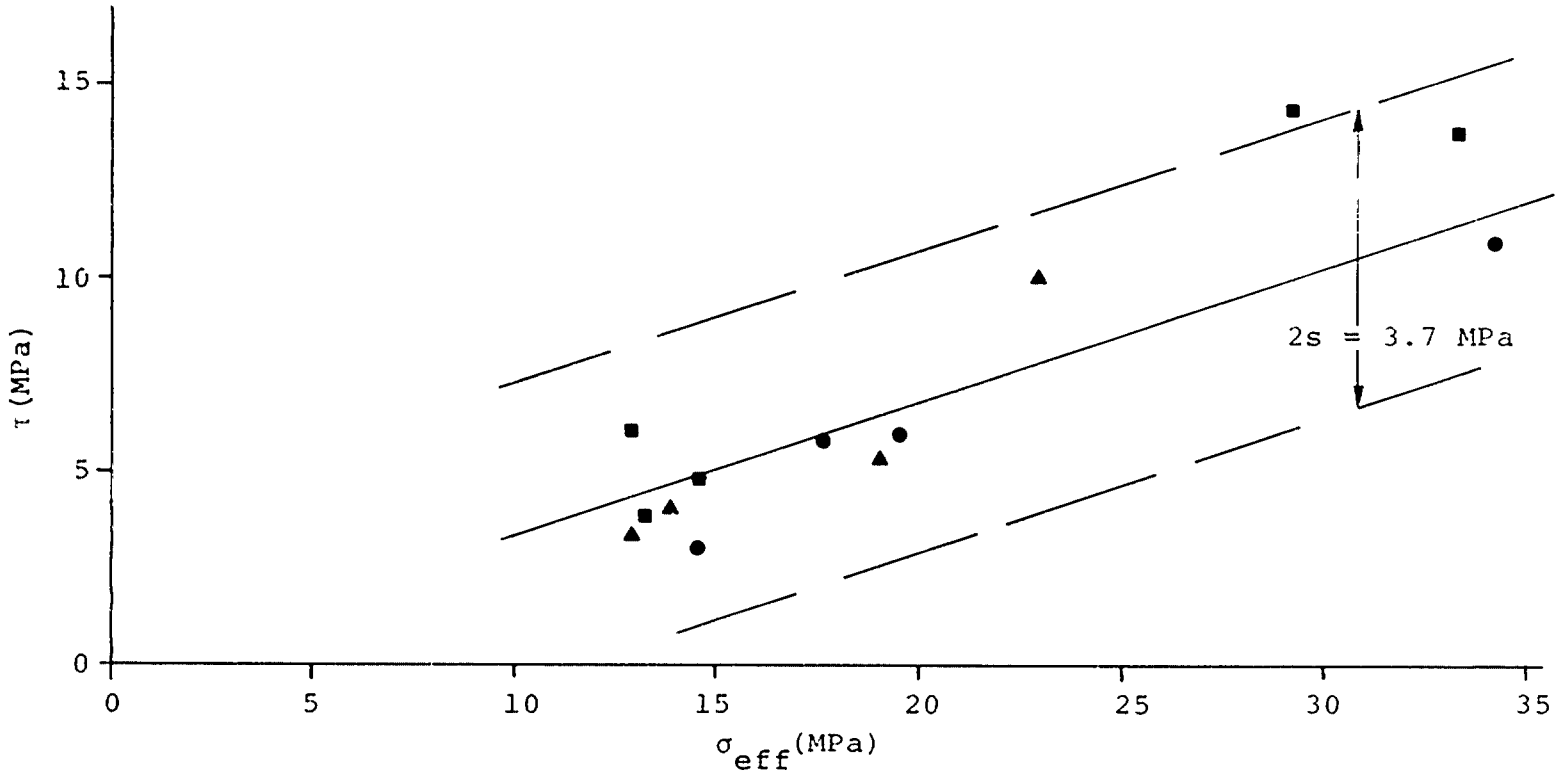

Figure 4.3 Friction data for wet sandstone recast in terms of σ_{eff}. Symbols as in Figure 3.2.

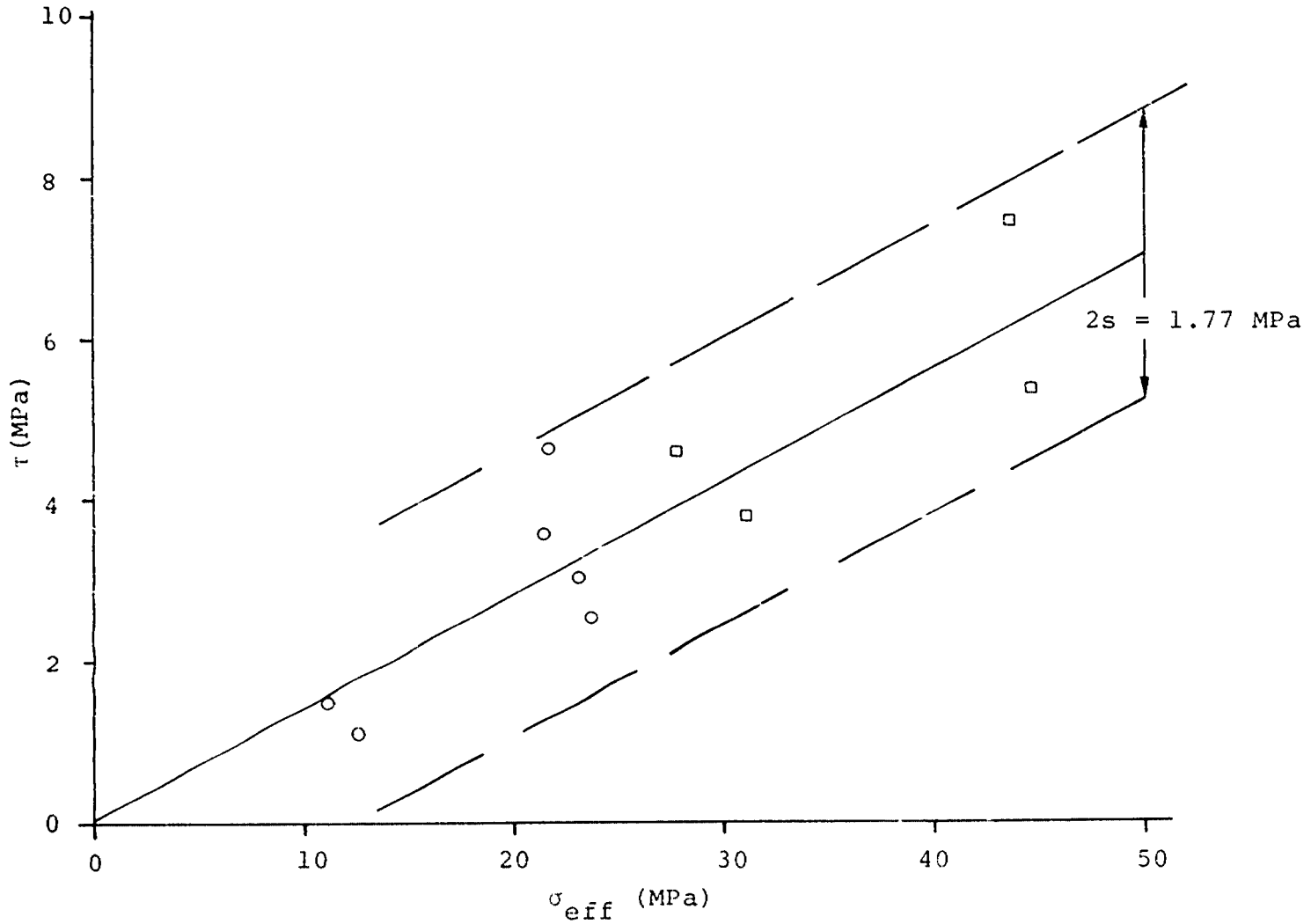

Figure 4.4 Friction data for limestone recast in terms of σ_{eff}. Symbols as in Figure 3.1.

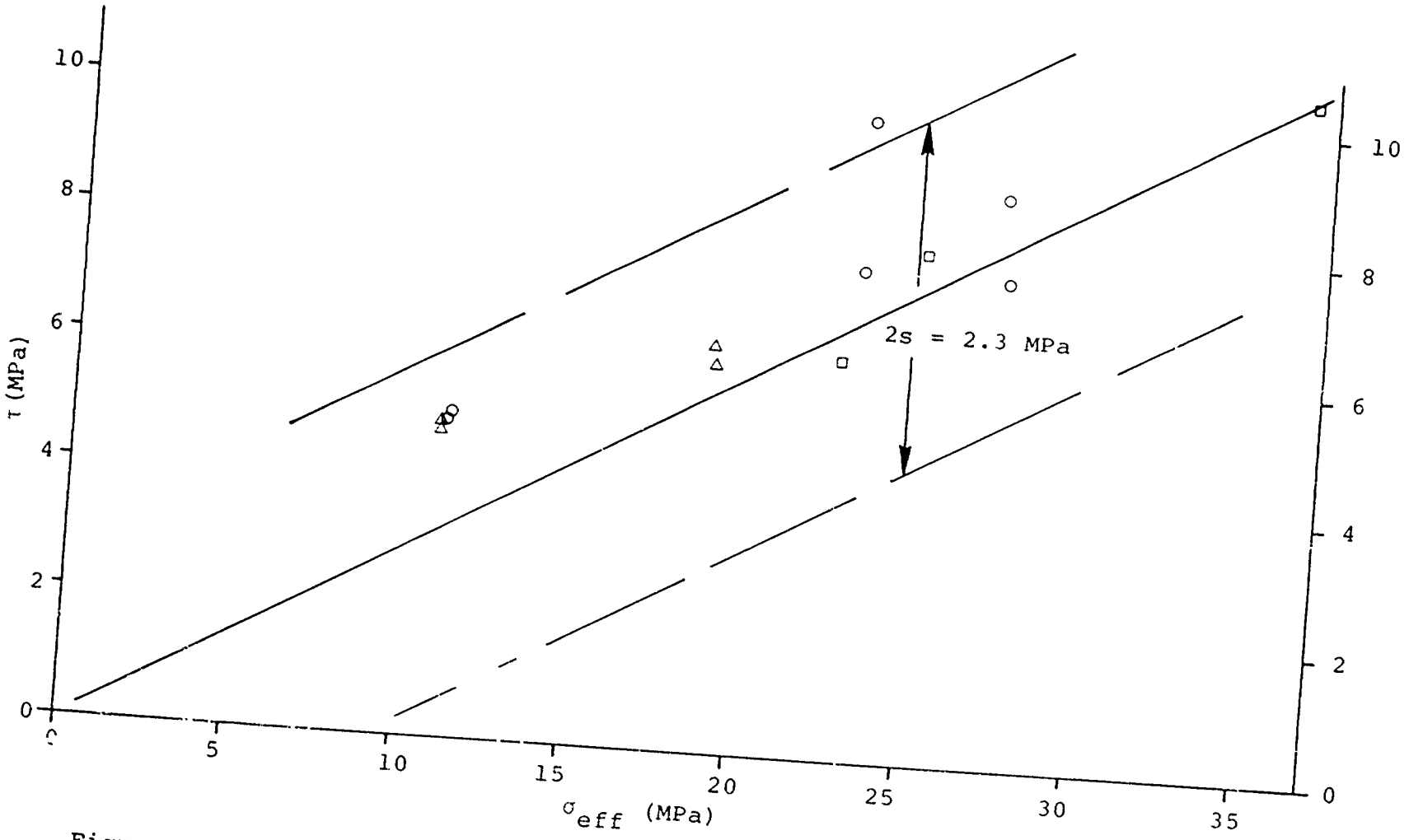

Figure 4.5 Friction data for sand-cement grout recast in terms of σ_{eff}. Symbols as in Figure 3.1.

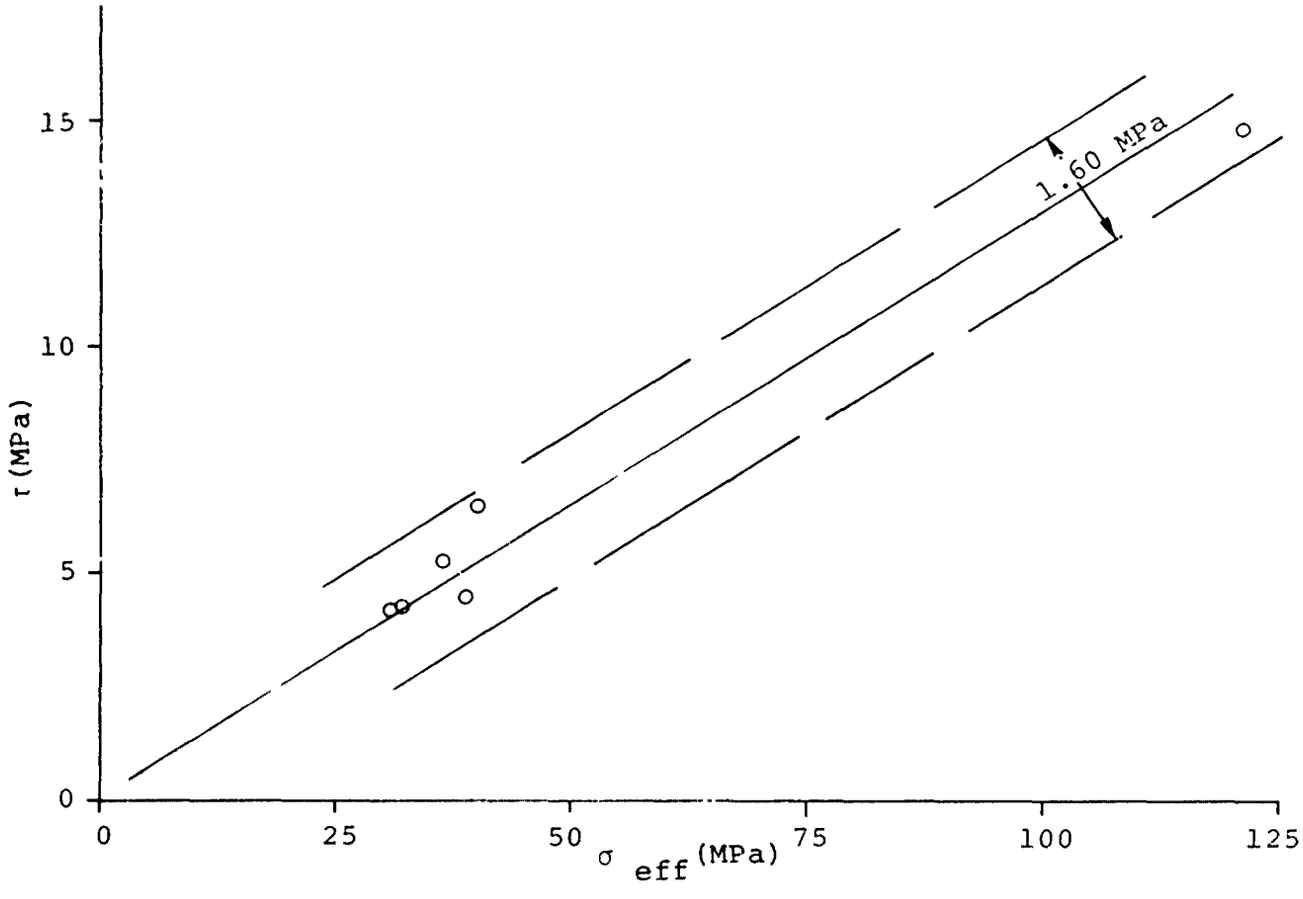

Figure 4.6 Friction data for bronze recast in terms of σ_{eff}. Symbols as in Figure 3.1.

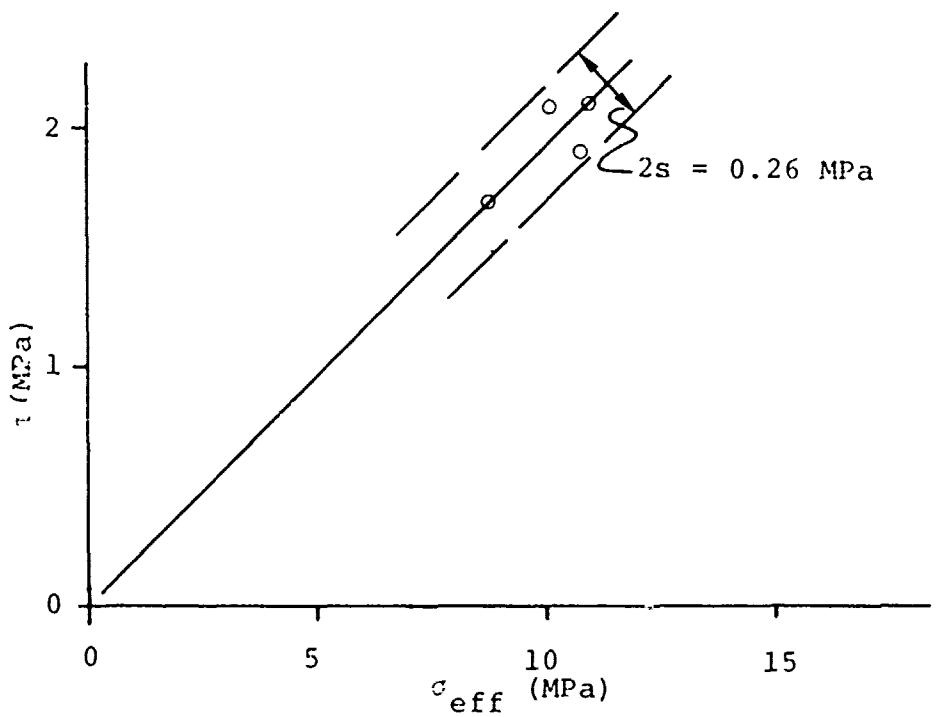

Figure 4.7 Friction data for teflon recast in terms of σ_{eff}. Symbols as in Figure 3.1.

The dependence of frictional behavior on the thermal conductivity of a small sample sliding on a large, high thermal conductivity wheel is not as would be expected from the analysis of Jaeger[3]. Jaeger's analysis indicates that the temperature at the sliding surface, and therefore, presumably the energy dissipation, for high sliding velocities will be virtually independent of the thermal conductivity of the small sliding sample, especially if the sample has a lower thermal conductivity than does the substrate. We have no explanation for the disparity between Jaeger's analysis and our results except that perhaps the mathematical model of Jaeger is too simplified to apply to the present results.

4.3 Variability of μ

We see from Table 4.1 a wide variation in the slope of τ with σ_{eff}. Values of μ as low as 0.13 (for bronze) and as high as 0.50 (for tuff) are seen.

In an investigation of static friction between soils and steel under low normal stresses, Potyondy[4] found that the ratio of the measured friction to the tangent of the angle of internal friction ranged from 0.39 to 0.93. Since τ/σ in Equation (2) approaches μ at low velocity and low normal stresses, it is appropriate to compare the present results with his. The angle of friction has been determined for four of the materials included in the present study. The values of tan ϕ are compared with those of μ in Table 4.3. The range of $\mu/\tan\phi$ seen in the present study is comparable to that of Potyondy[4]. More extensive work on a comprehensive suite of rocks would be necessary to determine the presence of a systematic relation between $\mu/\tan\phi$ and other material properties.

For the rocks and rock-like materials, we notice that those with a high percentage of potentially volatile material

Table 4.3 Sliding friction and internal friction for rocks and grout. ϕ is the angle of internal friction determined from the Mohr envelope for ultimate strength at low confining pressure.

Material	$\tan\phi$	μ	$\mu/\tan\phi$	Reference
TTR Tuff	0.58	0.50	0.86	(5)
Dakota Sandstone	0.53	0.39	0.74	(6)
Solenhofen Limestone	0.43	0.14	0.33	(7)
AVCO Grout	0.70	0.34	0.49	(8)

such as limestone, sand-cement grout and wet sandstone, have lower values of μ than do the dry rocks with no volatile components. This suggests that friction in wet or carbonaceous rocks is strongly affected by vapor formation. In the case of water-bearing rocks, the vapor is water vapor produced either by heating interstial water or by dehydrating hydrous minerals. In the case of limestone the volatile material must be CO_2 produced by thermal breakdown of $CaCO_3$.

It is, of course, dangerous to extrapolate the results for a small suite of rocks to the general case of all rocks. However, in view of the expense of obtaining such data, we feel that it is incumbent upon us at least to speculate. If we extrapolate these results to other rock types, we would anticipate that all carbonaceous rocks would have relatively low friction coefficients and that limestones might have lower coefficients than dolomites since higher temperatures are required to drive CO_2 out of dolomites than out of limestones. In the case of water-bearing rocks or porous rocks we would expect that any porous rock in a wet condition, whether saturated or unsaturated, would show appreciably lower coefficients for friction than the same rock in a dry condition. The number of rocks that we have looked at in the present study is insufficient to draw any conclusions as to the relative effectiveness of interstial water or bound water on frictional behavior of rocks.

Almost all soils contain appreciable amounts of water, as both bound water and interstial water. Because of this fact we would expect that low values of μ would be associated with soils. Furthermore, their low strength suggests that τ_o must be negligible for soils. In the absence of any direct data we would suggest a friction law for soils of the form

$$\tau \approx k \tan\phi \ \sigma \ e^{-c\sigma/600 \text{ MPa}\cdot\text{m/s}} \qquad (3)$$

where k is the ratio $\mu/\tan\phi$ suggested by Potyondy for that type of soil. In this form we have used a low value of ξ because of the low thermal conductivity of many soils.

4.4 Extrapolation of τ

In order to apply the present results to penetration problems of interest, we must extrapolate the data taken for sliding velocities of no more than 30 m/s at normal stresses below 100 MPa into the range of sliding velocities up to several 100 m/s and normal stresses in excess of 1 GPa. Such an extrapolation of two orders of magnitude or more in the product $c\sigma$ is clearly fraught with danger. As discussed below, we anticipate that the extrapolation will be valid. However, there are some results from previous investigations of metal-on-metal sliding friction at high velocities which indicate that there may be an increase in friction coefficients as we proceed to higher sliding velocities or higher normal stresses than included in the present investigation. These results are discussed by Bowden and Taber[9].

In summary, it is found that for high melting point metals, sliding on other metals, the coefficient of friction drops monotonically as sliding velocity is increased for a given normal force. However, for low melting point metals, the coefficient of friction first drops and then climbs once again to values near the zero-velocity value; in some cases it is noted that at even higher velocities the coefficient of friction once again begins to drop to very low values.

This phenomenon is explained by a change in the basic nature of the surface upon which the sliding occurs. At low velocities, where only moderate amounts of heat are generated at the sliding surface, all sliding occurs on small asperities on the surface. In other words, only a very small portion of the surfaces are actually in contact. As the sliding velocity

increases, the temperature of these contact points increases and very rapidly exceeds the melting point of the material. As the velocity increases further, the temperature of the molten material in the small contact areas increases, reducing the viscosity and thereby reducing the effective friction. However, if the sliding velocity continues to increase, eventually the area of contact begins to increase so that the energy loss in the small molten areas becomes very great. At some point the increase in area is more important than the increase in frictional energy. Thus, there is a larger area at lower temperature with a high viscosity and therefore a higher tangential force. Finally, after the entire gross sample area is molten, further increases in velocity increase the contact temperature and decrease the friction. This behavior is shown schematically in Figure 4.8.

The present results which show a maximum in tangential force with increasing speed at a given normal stress, might be supposed to lie in either the left-hand or right-hand portion where τ decreases as $c\sigma$ increases. Observations of sample surfaces and of the steel wheel surface after tests indicate that the entire contact area is covered with a thin layer of molten steel. This observation leads us to conclude that it is likely that coefficients of friction will continue to decrease as sliding speeds and normal stresses are increased. However, this conclusion is supported only by subjective observation of samples after a test, and not by objective or numerical data.

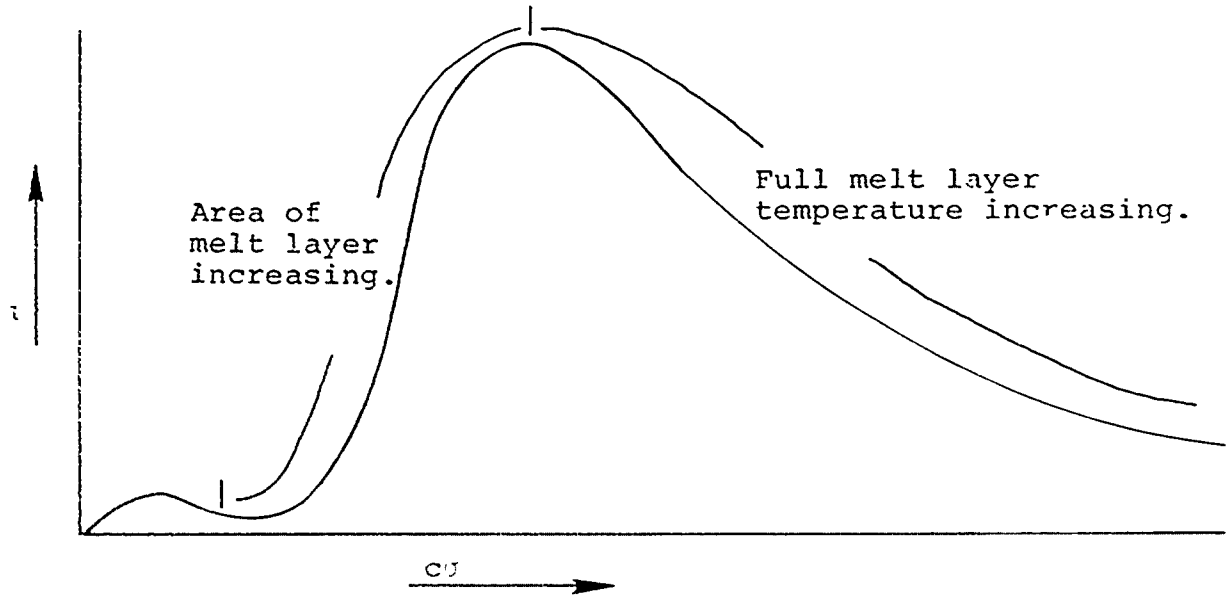

Figure 4.8 Behavior of coefficient of friction of a low melting-point metal sliding on steel at high velocities.

V. SUMMARY AND RECOMMENDATIONS

We have made measurements of frictional effects of several materials sliding on a dry steel wheel. Materials studied were welded TTR tuff, wet and dry Dakota sandstone, Solenhofen limestone, sand-cement grout, bronze and teflon. Sliding velocities were between 9.7 m/sec and 33 m/sec. Average normal stresses ranged from 8.5 MPa to 296 MPa.

The frictional behavior of all these materials can be expressed as $\tau = \mu\sigma\, e^{-c\sigma/\xi}$, where τ is the tangential stress, σ is the normal stress, c is the sliding velocity and μ and ξ are properties of the material. ξ is the same for all the rocks and the grout (2 GPa•m/s) but is higher for bronze (6.6 GPa•m/s) and lower for teflon (0.6 GPa•m/s). The value of ξ may be proportional to the thermal conductivity of the sample. Its units of energy flux suggest that it is related to the rate at which energy is lost from the sliding surface. μ is 0.50 to 0.39 for the dry, anhydrous rocks. It appears to be decreased by the presence of pore water, bound water or carbonate. (It is only 0.14 in limestone.)

Based on this data, it is tentatively proposed that friction between soil and steel might follow the relation $\tau = \kappa\tan\phi\ \sigma\ e^{-c\sigma/(600\ \mathrm{MPa\cdot m/s})}$. However, caution is suggested in using this relation since no measurements on soil were made.

Caution is also required in attempting to extrapolate this relation to velocities of hundreds of meters per second. Metal on metal friction can exhibit wide excursions in μ at speeds of that magnitude.

Based on this work we recommend the following work to validate the above relation for cases of interest to penetrator technology.

1. Measurements should be made with rocks at high sliding velocities (in excess of 100 m/s) and at higher normal stresses (above 100 MPa).

2. Measurements should be made with soils and with an extensive suite of rocks to determine if $\mu/\tan\phi$ can be related to other material properties.

3. Measurements with high initial temperatures should be undertaken. These measurements would be useful in quantifying the importance of melting in decreasing sliding friction.

4. Because of the asymmetry of these tests and of the penetration event, measurements should be made of steel sliding on rock.

5. Apparatus to make the above measurements at high velocities does not yet exist, hence, such an apparatus should be developed. All the recommended measurements could be accomplished in a rocket sled test program. By comparing the present results to the results of the recommended work, the sled program could probably be accomplished in 15 to 20 runs. Alternatively, special friction machines could be developed to make the measurements.

REFERENCES

1. E. S. Gaffney, 1975, "Rock/steel dynamic friction measurements," Systems, Science and Software Final Report No. SSS-R-75-2686 under Contract No. DNA001-75-C-0183 (DRAFT).

2. P. Hadala, letter to M. H. Wagner dated 1 March 1976.

3. J. C. Jaeger, 1942, "Moving sources of heat and the temperature at sliding contacts," Roy. Soc. N. So. Wales, J. and Proc. 76, 203-224.

4. J. G. Potyondy, 1961, "Skin friction between various soils and construction materials," Geotechnique 11, 339-353.

5. S. W. Butters, et al, 1976, "Field, laboratory and modeling studies of Mount Helen welded tuff for earth penetrator test evaluation," August 1976, Terra Tek, Salt Lake City, Utah.

6. D. K. Butler, et al, 1976, "Constitutive property investigations in support of full scale penetration tests: Report 1, Dakota sandstone, San Ysidro, N.M.," April 1976, (DRAFT) Technical Report, USAEWES, Vicksburg, MS.

7. J. Handin, 1966, "Strength and ductility," Ch. 11 in S. P. Clark, Jr. (ed.) Handbook of Physical Constants. Geol. Soc. Am. Memoir 97, pp. 223-290.

8. D. K. Butler, 1975, letter report from WES to Maj. T. Stong (DNA) dated 16 December 1975.

9. F. P. Bowden and D. Tabor, 1964, The Friction and Lubrication of Solids, Part II, Clarendon Press, Oxford.

DISTRIBUTION LIST

DEPARTMENT OF DEFENSE

Director
Defense Advanced Rsch. Proj. Agency
ATTN: Technical Library

Director
Defense Civil Preparedness Agency
ATTN: Admin. Officer

Defense Documentation Center
12 Cy ATTN: TC

Director
Defense Intelligence Agency
ATTN: DI-7E
ATTN: DB-4C, Edward O'Farrell
ATTN: Charles A. Fowler
ATTN: Technical Library
ATTN: DT-2, Wpns. & Sys. Div.

Director
Defense Nuclear Agency
ATTN: SPAS
ATTN: STSI Archives
ATTN: DDST
3 Cy ATTN: STTL, Tech. Library
5 Cy ATTN: SPSS

Dir. of Defense Rsch. & Engineering
ATTN: S&SS(OS)

Commander
Field Command, DNA
ATTN: FCPR

Director
Interservice Nuclear Weapons School
ATTN: Document Control

Director
Joint Strat. Tgt. Planning Staff, JCS
ATTN: STINFO Library

Chief
Livermore Division, FC, DNA
ATTN: FCPRL

DEPARTMENT OF THE ARMY

Dep. Chief of Staff for Rsch. Dev. & Acq.
ATTN: DAMA(CS), MAJ A. Gleim
ATTN: Technical Library
ATTN: DAMA-CSM-N, LTC G. Ogden

Chief of Engineers
2 Cy ATTN: DAEN-MCE-D
2 Cy ATTN: DAEN-RDM

Dep. Chief of Staff for Ops. & Plans
ATTN: Technical Library
ATTN: Dir. of Chem. & Nuc. Ops.

Chief
Engineer Strategic Studies Group
ATTN: DAEN-FES

DEPARTMENT OF THE ARMY (Continued)

Commander
Frankford Arsenal
ATTN: L. Baldini

Project Manager
ATTN: E. J. Linddsey

Commander
Harry Diamond Laboratories
ATTN: DRXDO-RBH, James H. Gwaltney
ATTN: DRXDO-NP

Commander
Picatinny Arsenal
ATTN: Ray Moesner
ATTN: B. Shulman (DR-DAR-L-C-FA)
ATTN: SMUPA-AD-D-A
ATTN: Marty Margolin
ATTN: Jerry Pental
ATTN: SMUPA-AD-D-A-7
ATTN: SMUPA-AD-D-M
ATTN: Paul Harris
ATTN: Ernie Zimpo
ATTN: Technical Library
ATTN: P. Angelloti

Commander
Redstone Scientific Information Ctr.
ATTN: Chief, Documents

Commander
U.S. Army Armament Command
ATTN: Tech. Library

Director
U.S. Army Ballistic Research Labs.
ATTN: G. Roecker
ATTN: A. Ricchiazzi
ATTN: J. H. Keefer, DRDAR-BLE
ATTN: DRXBR-X
ATTN: G. Grabarek
ATTN: DRXBR-TB
ATTN: J. W. Apgar
2 Cy ATTN: Tech. Lib., Edward Baicy

Commander and Director
U.S. Army Cold Region Res. Engr. Lab.
ATTN: G. Swinzow

Commander
U.S. Army Comb. Arms Combat Dev. Acty.
ATTN: LTC G. Steger
ATTN: LTC Pullen

Commander
U.S. Army Engineer Center
ATTN: ATSEN-SY-L

Division Engineer
U.S. Army Engineer Div., Huntsville
ATTN: HNDED-SR

DEPARTMENT OF THE ARMY (Continued)

Division Engineer
U.S. Army Engineer Div., Missouri Rvr.
ATTN: Tech. Library

Commandant
U.S. Army Engineer School
ATTN: ATSE-TEA-AD
ATTN: ATSE-CTD-CS

Director
U.S. Army Engr. Waterways Exper. Sta.
ATTN: D. K. Butler
ATTN: Behzad Rohani
ATTN: Guy Jackson
ATTN: William Flathau
ATTN: John N. Strange
ATTN: P. Hadala
ATTN: Leo Ingram
ATTN: Tech. Library

Commander
U.S. Army Mat. & Mechanics Rsch. Ctr.
ATTN: Tech. Library

Commander
U.S. Army Materiel Dev. & Readiness Cmd.
ATTN: Tech. Library

Director
U.S. Army Materiel Sys. Analysis Acty.
ATTN: Joseph Sperazza

Commander
U.S. Army Missile Command
ATTN: W. Jann
ATTN: F. Fleming
ATTN: J. Hogan

Commander
U.S. Army Mobility Equip. R & D Ctr.
ATTN: STSFB-XS
ATTN: STSFB-MW
ATTN: Tech. Library

Commander
U.S. Army Nuclear Agency
ATTN: Tech. Library
ATTN: Doc. Con.

Commander
U.S. Army Training and Doctrine Comd.
ATTN: LTC Auveduti, COL Enger
ATTN: LTC J. Foss

Commandant
U.S. Army War College
ATTN: Library

U.S. Army Mat. Comd. Proj. Mngr. for Nuc. Munitions
ATTN: DRCPM-NUC

DEPARTMENT OF THE NAVY

Chief of Naval Operations
ATTN: OP 982, LTC Dubac
ATTN: OP 982, LCDR Smith
ATTN: Code 604C3, Robert Piacesi
ATTN: OP 982, CAPT Toole

DEPARTMENT OF THE NAVY (Continued)

Chief of Naval Research
ATTN: Technical Library

Officer-In-Charge
Civil Engineering Laboratory
ATTN: R. J. Odello
ATTN: Technical Library

Commandant of the Marine Corps
ATTN: POM

Commanding General
Development Center
ATTN: CAPT Hartneady
ATTN: LTC Gapenski

Commander
Naval Air Systems Command
ATTN: F. Marquardt

Commanding Officer
Naval Explosive Ord. Disposal Fac.
ATTN: Code 504, Jim Petrousky

Commander
Naval Facilities Engineering Command
ATTN: Technical Library

Superintendent (Code 1424)
Naval Postgraduate School
ATTN: Code 2124, Tech. Rpts. Librarian

Director
Naval Research Laboratory
ATTN: Code 2600, Tech. Lib.

Commander
Naval Sea Systems Command
ATTN: ORD-033
ATTN: SEA-9931G

Commander
Naval Surface Weapons Center
ATTN: M. Kleinerman
ATTN: Code WA501, Navy Nuc. Prgms. Off.
ATTN: WX21, Tech. Lib.

Commander
Naval Surface Weapons Center
Dahlgren Laboratory
ATTN: Technical Library

Commander
Naval Weapons Center
ATTN: Carl Austin
ATTN: Code 533, Tech. Lib.

Commanding Officer
Naval Weapons Evaluation Facility
ATTN: Tech. Lib.

Director
Strategic Systems Project Office
ATTN: NSP-43, Tech. Lib.

DEPARTMENT OF THE NAVY (Continued)

Director
Office of Naval Research
Branch Office
ATTN: E. H. Weinburg

DEPARTMENT OF THE AIR FORCE

AF Armament Laboratory, AFSC
ATTN: Masey Valentine
3 Cy ATTN: John Collins, AFATL/DLYV

AF Institute of Technology, Au
ATTN: Library AFIT, Bldg. 640, Area B

AF Weapons Laboratory, AFSC
ATTN: SUL

Headquarters
Air Force Systems Command
ATTN: Technical Library

Commander
Armament Development & Test Center
ATTN: Tech. Library

Assistant Secretary of the Air Force
Research and Development
ATTN: Col R. E. Steere

Deputy Chief of Staff
Research and Development
ATTN: Col J. L. Gilbert

Commander
Foreign Technology Division, AFSC
ATTN: NICD Library

Hq. USAF/IN
ATTN: INATA

Hq. USAF/RD
ATTN: RDPM

Oklahoma State University
Fld. Off. for Wpns. Effectivensss
ATTN: Edward Jackett

Commander
Rome Air Development Center, AFSC
ATTN: EMTLD, Doc. Library

SAMSO/RS
ATTN: RSS

ENERGY RESEARCH AND DEVELOPMENT ADMINISTRATION

Division of Military Application
ATTN: Doc. Control for Test Office

University of California
Lawrence Livermore Laboratory
ATTN: Jerry Goudreau
ATTN: Tech. Info. Dept. L-3
ATTN: Mark Wilkins, L-504

Los Alamos Scientific Laboratory
ATTN: Doc. Con. for Tom Dowler
ATTN: Doc. Con. for Reports Lib.

ENERGY RESEARCH & DEVELOPMENT ADMINISTRATION (Continued)

Sandia Laboratories
Livermore Laboratory
ATTN: Doc. Con. for Tech. Lib

Sandia Laboratories
ATTN: Doc. Con. for 3141 Sandia Rpt. Coll.
ATTN: Doc. Con. for Walter Herrmann
ATTN: Doc. Con. for W. Altsmeirer
ATTN: Doc. Con. for John Colp
ATTN: Doc. Con. for John Keizur
ATTN: Doc. Con. for William Caudle
ATTN: Doc. Con. for William Patterson

U.S. Energy Rsch. & Dev. Admin.
Albuquerque Operations Office
ATTN: Doc. Con. for Tech. Lib.

U.S. Energy Rsch. & Dev. Admin.
Division of Headquarters Services
ATTN: Doc. Con. for Class. Tech. Lib.

U.S. Energy Rsch. & Dev. Admin.
Nevada Operations Office
ATTN: Doc. Con. for Tech. Lib.

OTHER GOVERNMENT SERVICES

NASA
Ames Research Center
ATTN: Robert W. Jackson

Office of Nuclear Reactor Regulation
Nuclear Regulatory Commission
ATTN: Robert Heineman
ATTN: Lawrence Shao

DEPARTMENT OF DEFENSE CONTRACTORS

Aerospace Corporation
ATTN: Tech. Info. Services

Agbabian Associates
ATTN: M. Agbabian

Applied Theory, Inc.
2 Cy ATTN: John G. Trulio

Avco Research & Systems Group
ATTN: David Henderson
ATTN: Res. Lib. A830, Rm. 7201
ATTN: Pat Grady

Battelle Memorial Institute
ATTN: Technical Library

The BDM Corporation
ATTN: Technical Library

The Boeing Company
ATTN: Aerospace Library

California Research & Technology, Inc.
ATTN: Ken Kreyenhagen
ATTN: Technical Library

Civil/Nuclear Systems Corp.
ATTN: Robert Crawford

DEPARTMENT OF DEFENSE CONTRACTORS (Continued)

EG&G, Inc.
Albuquerque Division
ATTN: Technical Library

Engineering Societies Library
ATTN: Ann Mott

General Dynamics Corp.
Pomona Division
ATTN: Keith Anderson

General Electric Company
TEMPO-Center for Advanced Studies
ATTN: DASIAC

Georgia Institute of Technology
ATTN: S. V. Hanagud
ATTN: L. W. Rehfield

Honeywell, Incorporated
Defense Systems Division
ATTN: T. N. Helvig

Institute for Defense Analyses
ATTN: IDA Librarian, Ruth S. Smith

Kaman AviDyne
Division of Kaman Sciences Corp.
ATTN: Technical Library

Kaman Sciences Corp.
ATTN: Library

Lockheed Missiles & Space Co., Inc.
ATTN: Technical Library
ATTN: M. Culp

Lockheed Missiles & Space Co., Inc.
ATTN: Tech. Info. Ctr. D/Coll.

Martin Marietta Aerospace
Orlando Division
ATTN: Al Cowen
ATTN: M. Anthony
ATTN: H. McQuaig

Merritt Cases, Inc.
ATTN: Technical Library
ATTN: J. L. Merritt

University of New Mexico
Dept. of Campus Security and Police
ATTN: G. E. Triandafalidis

Newmark, Nathan M.
Consulting Engineering Services
University of Illinois
ATTN: Nathan M. Newmark

Pacifica Technology
ATTN: R. Bjork
ATTN: G. Kent

Physics International Co.
ATTN: Doc. Con. for Dennis Orphal
ATTN: Doc. Con. for Tech. Lib.
ATTN: Doc. Con. for Larry A. Behrmann
ATTN: Doc. Con. for Charles Godfrey

DEPARTMENT OF DEFENSE CONTRACTORS (Continued)

R & D Associates
ATTN: Paul Rausch
ATTN: Henry Cooper
ATTN: J. G. Lewis
ATTN: Harold L. Brode
ATTN: Arlen Fields
ATTN: William B. Wright, Jr.
ATTN: Technical Library
ATTN: Cyrus P. Knowles

The Rand Corporation
ATTN: Technical Library

Science Applications, Inc.
ATTN: Technical Library

Stanford Research Institute
ATTN: George R. Abrahamson

Systems, Science and Software, Inc.
ATTN: Technical Library
ATTN: Robert Sedgewick
ATTN: E. S. Gaffney

Terra Tek, Inc.
ATTN: Technical Library

TRW Systems Group
ATTN: Tech. Info. Center/S-1930
ATTN: Peter K. Dai, R1/2170

TRW Systems Group
ATTN: E. Y. Wong, 527/712

Weidlinger Assoc. Consulting Engineers
ATTN: Melvin L. Baron
ATTN: J. M. McCormick

Weidlinger Assoc. Consulting Engineers
ATTN: J. Isenberg

General Electric Co.
ATTN: L. P. Sudrea

Communications Satellite Corp.
ATTN: Jim Petrousky